Molybdenum and Tungsten η^1- and η^2-Aldehyde Complexes

Danae M. Schuster, Peter S. White, and Joseph L. Templeton*

W. R. Kenan, Jr., Laboratory, Department of Chemistry, The University of North Carolina, Chapel Hill, North Carolina 27599-3290

Received October 27, 1999

A series of molybdenum(II) and tungsten(II) aldehyde complexes of the type [{Tp}M(CO)(RC≡CMe)(η^1/η^2-O═CHR′)][BAr′$_4$] ({Tp} = Tp′, Tp; R = Ph, Me) (**5**−**8**) has been prepared for the purpose of investigating σ/π-aldehyde binding. The aldehyde complexes were generated by protonation of the methyl complexes {Tp}M(CO)(RC≡CMe)Me (**1**−**4**) with HBAr′$_4$·OEt$_2$ (HBAr′$_4$ = tetrakis[3,5-bis(trifluoromethyl)phenyl]borate), loss of methane, and addition of aldehyde (acetaldehyde, propionaldehyde, pivaldehyde, acrolein, *trans*-crotonaldehyde, methacrolein, benzaldehyde, *p*-tolualdehyde, or *p*-anisaldehyde). The aldehyde complexes exhibit varying σ/π-aldehyde coordination depending on the aldehyde, the metal, and the metal's ancillary ligands. Within the series, π-binding is observed only in the electron-rich and sterically less encumbered Tp tungsten complexes (**7**), where the π/σ-isomer ratio is dependent on the nature of the aldehyde. In contrast, aldehydes are σ-bound in the less electron-rich Tp molybdenum complexes (**8**) and in the more sterically encumbered Tp′ tungsten and molybenum complexes **5** and **6**. Variable-temperature FTIR measurements show that the π/σ-isomer ratio in the Tp tungsten complexes (**7**) increases as the temperature is lowered.

Introduction

The rates and stereoselectivities of reactions of organic carbonyls can be altered significantly by coordination to Lewis acids.[1−4] Central to the reactivity of organic carbonyls coordinated to transition metal Lewis acids is whether the carbonyl binding mode is π or σ (Scheme 1).[5] A π-coordinated organic carbonyl coordinates to the metal fragment through the carbonyl π-orbital. As a consequence of substantial back-bonding from the metal dπ-orbital to the organic carbonyl π^*-orbital in π-complexes, the C═O absorbance of the organic carbonyl is lowered significantly in the IR, and both the carbonyl carbon (*C*═O) in ^{13}C NMR and the aldehydic proton (C*H*O) in ^{1}H NMR are shifted upfield relative to free organic carbonyls.[6] Similar spectral data for σ-bound carbonyls more closely resemble free organic carbonyls.[1b]

Scheme 1

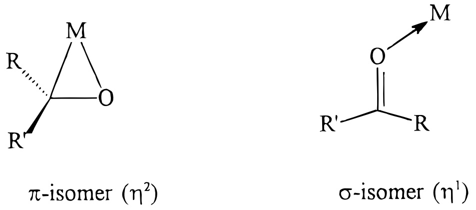

Several factors affect the mode of coordination of organic carbonyls to transition metal Lewis acids: the

---

[1] For reviews, see: (a) Shambayati, S.; Schreiber, S. L. In *Comprehensive Organic Synthesis*; Trost, B. M., Editor-in-Chief; Fleming, I., Deputy Editor-in-Chief; Schrieber, S. L., Volume Editor; Pergamon: New York, 1991; Vol 1, Chapter 1.10. (b) Huang, Y. H.; Gladysz, J. A. *J. Chem. Educ.* **1988,** *65,* 298, and references therein.

[2] For main group Lewis acids, see: (a) Shambayati, S.; Crowe, W. E.; Stuart, S. L. *Angew. Chem., Int. Ed. Engl.* **1990,** *29,* 256. (b) Reetz, M. T.; Hüllmann, M.; Massa, W.; Berger, S.; Rademacher, P.; Heymanns, P. *J. Am. Chem. Soc.* **1986**, *108*, 2405. (c) Raber, D. J.; Raber, N. K.; Chandrasekhar, J.; Schleyer, P. von R. *Inorg. Chem.* **1984**, *23*, 4076. (d) LePage, T. J.; Wiberg, K. B. *J Am. Chem. Soc.* **1988**, *110*, 6642. (e) Hunt, I. R.; Rogers, C.; Woo, S.; Rauk, F.; Keay, B. A. *J. Am. Chem. Soc.* **1995**, *117*, 1049. (f) Denmark, S. E.; Almstead, N. G. *J. Am. Chem. Soc.* **1993**, *115*, 3133.

[3] For transition metal Lewis acids, see: (a) Bonnesen, P. V.; Puckett, C. L.; Honeychuck, R. V.; Hersh, W. H. *J. Am. Chem. Soc.* **1989,** *111*, 6070. (b) Foxman, V. M.; Klemarczyk, P. T.; Liptrot, R. E.; Rosenblum, M. *J. Organomet. Chem.* **1980**, *187*, 253. (c) Birk, R.; Berke, H.; Hund, H.; Evertz, K.; Huttner, G.; Zsolnai, L. *J. Organomet. Chem.* **1988**, *342*, 67. (d) Cicero, R. L.; Prostasiewicz, J. D. *Organometallics* **1995**, *14*, 4792.

[4] For chiral-at-metal transition metal Lewis acids, see: (a) Brunner, H.; Aclasis, J.; Langer, M.; Steger, W. *Angew. Chem., Int. Ed. Engl.* **1974**, *13*, 810. (b) Merrifield, J. H.; Strouse, C. E.; Gladysz, J. A. *Organometallics* **1982**, *1*, 1204. (c) Huang, Y.-H.; Niedercorn, F.; Arif, A. M.; Gladysz, J. A. *J. Organomet. Chem.* **1990**, *383*, 213. (d) Brookhart, M.; Liu, Y. *Organometallics* **1989**, *8*, 1572. (e) Dalton, D. M.; Fernández, J. M.; Emerson, K.; Larsen, R. D.; Arif, A. M.; Gladysz, J. A. *J. Am. Chem. Soc.* **1990**, *112*, 9198. (f) Dalton, D. M.; Fernández, J. M.; Emerson, K.; Larsen, R. D.; Arif, A. M.; Gladysz, J. A. *J. Chem. Soc., Chem. Commun.* **1988**, 37. (g) Garner, C. M.; Fernández, J. M.; Gladysz, J. A. *Tetrahedron Lett.* **1989**, 3931.

[5] For a discussion of linkage isomerism see: Burmeister, J. L. *Coord Chem. Rev.* **1968**, *3*, 225.

[6] Wang, Y.; Agbossou, F.; Dalton, D. M.; Liu, Y.; Arif, A. M.; Gladysz, J. A. *Organometallics* **1993**, *12*, 2699.

[7] Generally, ketones are σ-bound to metal fragments because they are bulkier and less π-acidic than aldehydes. See: Delbeca, F.; Sautet, P. *J. Am. Chem. Soc.* **1992**, *114*, 2446.

[8] For π-bound ketones, see: (a) Klein, D. P.; Dalton, D. M.; Méndez, N. Q.; Arif, A. M.; Gladysz, J. A. *J. Organomet. Chem.* **1991**, *412*, C7. (b) Countryman, R.; Penfold, B. R. *J. Chem. Soc., Chem. Commun.* **1971**, 1598. (c) Okuda, J.; Herberich, G. E. *Organometallics* **1987**, *6*, 2331. (d) Clark, B.; Green, M.; Osborn, R. B. L.; Stone, F. G. A. *J. Chem. Soc. A* **1968**, 167. (e) Bryan, J. C.; Mayer, J. M. *J. Am. Chem. Soc.* **1990**, *112*, 2298. (f) Gambarotta, S.; Pasquali, M.; Floriani, C.; Chiesi-Villa, A.; Guastini, C. *Inorg. Chem.* **1981**, *20*, 1173. (g) Hill, J. E.; Fanwick, P. E.; Rothwell, I. P. *Organometallics* **1992**, *11*, 1771. (h) Tsou, T. T.; Huffman, J. C.; Kochi, J. K. *Inorg. Chem.* **1979**, *18*, 2311.

10.1021/om990864x CCC: $19.00

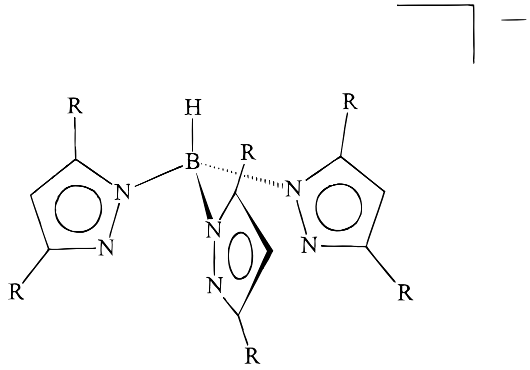

Figure 1. Hydridotris(pyrazolyl)borate ligands: Tp = hydridotris(1-pyrazolyl)borate (R = H; cone angle = 184°); Tp′ = hydridotris(3,5-dimethylpyrazolyl)borate (R = Me; cone angle = 224°).

nature of the organic carbonyl,[7−9] the metal and its oxidation state,[7,10,11] and the steric imposition of the metal's ancillary ligands.[12] In this paper, a series of tungsten and molybdenum hydridotris(1-pyrazolyl)borate (Tp) and hydridotris(3,5-dimethylpyrazolyl)borate (Tp′)[13] aldehyde complexes have been synthesized in order to probe the effect these factors have on aldehyde binding.[14] Lewis acids with the Tp′ ligand are electron-rich and sterically encumbered relative to Lewis acidic Tp complexes (Figure 1). Tungsten complexes are more electron-rich than their molybdenum analogues, as reflected in comparable ν(C$\equiv$O) values (vide infra), and comparison provides a probe for electronic factors in metal−aldehyde binding.

We report (1) syntheses of saturated, α,β-unsaturated, and aromatic aldehyde complexes of Tp′ and Tp molybdenum and tungsten Lewis acids, (2) the X-ray structure of a *trans*-crotonaldehyde complex, [Tp′W(CO)(PhC$\equiv$CMe)(η^1−O=CHCH=CHMe)][BAr′$_4$] (**5e**), and (3) variable-temperature FTIR spectra of [TpW(CO)(MeC$\equiv$CMe)(η^1/η^2-*p*-O=CHC$_6$H$_4$OMe)][BAr′$_4$] (**7i**).

Results and Discussion

Chart 1. Structures of Tungsten and Molybdenum Methyl Complexes

1: M = W; ν(C$\equiv$O) = 1874 cm^{-1}
2: M = Mo; ν(C$\equiv$O) = 1892 cm^{-1}
3: M = W; ν(C$\equiv$O) = 1884 cm^{-1}
4: M = Mo; ν(C$\equiv$O) = 1896 cm^{-1}

Chart 2. Structures of Tungsten and Molybdenum Aldehyde Complexes

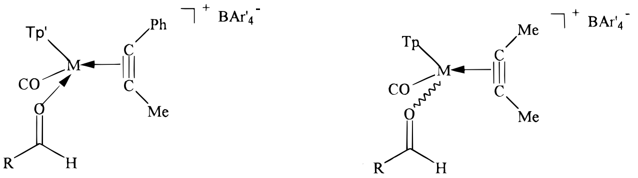

5: M = W; σ-bound
6: M = Mo; σ-bound
7: M = W; σ- or π-bound
8: M = Mo; σ-bound

Synthesis of Aldehyde Complexes. Protonation of the methyl complexes **1**−**4**[14a] (Chart 1) with HBAr′$_4$·OEt$_2$[15] at −78 °C,[16] followed by addition of acetaldehyde, propionaldehyde, pivaldehyde, acrolein, *trans*-crotonaldehyde, methacrolein, benzaldehyde, *p*-tolualdehyde, or *p*-anisaldehyde generated the aldehyde complexes **5**−**8** (eq 1, Chart 2). To avoid alkyne rotamer complications in Tp complexes,[14a] the 2-butyne Lewis acid precursors **3** and **4** were used to synthesize Tp aldehyde complexes. To avoid counterion interference, HBAr′$_4$·OEt$_2$ is the preferred acid. In addition, the [BAr′$_4$]$^-$ salts are more stable, easier to recrystallize, and exhibit higher solubility in low-polarity solvents than [BF$_4$]$^-$ analogues. The aldehyde complexes were obtained as analytically pure crystals in 69−93% yields after workup.

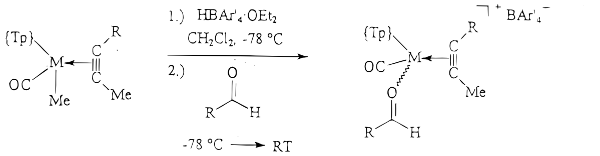

(1)

1 - 4

5 - 8

σ- or π-bound

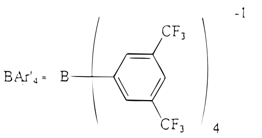

tetrakis[3,5-bis(trifluoromethyl)phenyl]borate

Saturated Aldehyde Complexes. Within the series, π-binding is only observed in the Tp tungsten products (**7**). The metal C$\equiv$O absorbances in the IR spectra and the downfield shift observed for the aldehyde carbonyl carbon (C=O) in the ^{13}C NMR spectra of Tp′ tungsten products **5a**−**c** are typical of Tp′ σ-complexes (Table 1).[14] π-Isomers were not detected in either ambient temper-

---

[9] Aldehyde complexes of the [CpRe(NO)(PPh$_3$)]$^+$ fragment exist as a mixture of σ- and π-isomers: (a) Garner, C, M.; Méndez, N. Q.; Kowalczyk, J. J.; Fernández, J. M.; Emerson, K.; Larsen, R. D.; Gladysz, J. A. *J. Am. Chem. Soc.* **1990**, *112*, 5146. (b) Agbossou, F.; Ramsden, J. A.; Huang, Y.; Arif, A.; Gladysz, J. A. *Organometallics* **1992**, *11*, 693. (c) Méndez, N. Q.; Seyler, J. W.; Arif, A. M.; Gladysz, J. A. *J. Am. Chem. Soc.* **1993**, *115*, 2323. (d) Boone, B. J.; Klein, D. P.; Seyler, J. W.; Méndez, N. Q.; Arif, A. M.; Gladysz, J. A. *J. Am. Chem. Soc.* **1996**, *118*, 2411.

[10] (a) Spera, M. L.; Chen, H.; Moody, M. W.; Hill, M. M.; Harman, W. D. *J. Am. Chem. Soc.* **1997**, *119*, 12772. (b) Harman, W. D.; Sekine, M.; Taube, H. *J. Am. Chem. Soc.* **1988**, *110*, 2439. (c) Harman, W. D.; Dobson, J. C.; Taube, H. *J. Am. Chem. Soc.* **1989**, *111*, 3061. (d) Harman, W. D.; Fairlie, D. P.; Taube, H. *J. Am. Chem. Soc.* **1986**, *108*, 8223.

[11] Powell, D. W.; Lay, P. A. *Inorg. Chem.* **1992**, *31*, 3542.

[12] Faller, J. W.; Ma, Y. *J. Am. Chem. Soc.* **1991**, *113*, 1579.

[13] For related hydridotris(3,5-dimethylpyrazolyl)borate ligand (Tp′) complexes, see: (a) Feng, S. G.; Templeton, J. L. *Organometallics* **1992**, *11*, 1295. (b) Gunnoe, T. B.; White, P. S.; Templeton, J. L. *J. Am. Chem. Soc.* **1996**, *118*, 6916. (c) Rusik, C. A.; Collins, M. A.; Gamble, A. S.; Tonker, T. L.; Templeton, J. L. *J. Am. Chem. Soc.* **1989**, *111*, 2550. (d) Collins, M. A.; Feng, S. G.; White, P. S.; Templeton, J. L. *J. Am. Chem. Soc.* **1992**, *114*, 3771.

[14] Similar studies involving ketones binding to these Lewis acids have been reported: (a) Schuster, D. M.; Templeton, J. L. *Organometallics* **1998**, *17*, 2707. (b) Caldarelli, J. L.; Wagner, L. E.; White, P. S.; Templeton, J. L. *J. Am. Chem. Soc.* **1994**, *116*, 2878.

[15] (a) Nishida, H.; Takada, N.; Yoshimura, M.; Sonoda, T.; Kobayashi, H. *Bull. Chem. Soc. Jpn.* **1984**, *57*, 2600. (b) Brookhart, M.; Grant, B.; Volpe, A. F. *Organometallics* **1992**, *11*, 3920.

[16] Protonation of the methyl complex at −78 °C generates a methylene chloride intermediate, where the methylene chloride is displaced upon addition of the aldehyde. See: Fernández, J. M.; Gladysz, J. A. *Organometallics* **1989**, *8*, 207.

Table 1. Selected Data for Saturated Aldehyde Complexes [{Tp}W(CO)(R′C≡CMe)(O=CHR)][BAr′$_4$] (See Chart 2)

compound	R	mode (π/σ)[a]	IR, ν(C≡O) (cm^{-1}, CH$_2$Cl$_2$)	^{1}H NMR O=C*H*R (ppm)[b]	^{13}C NMR O=*C*HR (ppm)[b]
acetaldehyde	Me			9.74	199.7
5a (Tp′W)	Me	σ	1939	7.90	210.4
7a (TpW)	Me	π	2042	5.93	98.4
propionaldehyde	Et			9.75	202.8
5b (Tp′W)	Et	σ	1939	7.90	214.9
7b (TpW)	Et	π	2043	5.80	103.8
pivaldehyde	^{t}Bu			9.44	204.0
5c[c] (Tp′W)	^{t}Bu	σ	1938[d]	7.64	219.0
7c (TpW)	^{t}Bu	π/σ (11:89)	2046/1954	7.29	210.9[e]

[a] IR detection limit: 3%. [b] In CD$_2$Cl$_2$. [c] See ref 14b. [d] KBr value. [e] ^{13}C NMR spectrum obtained at −20 °C.

ature IR or NMR spectra of **5a**−**c**. The signal for the aldehydic proton (C*H*O) in ^{1}H NMR is surprisingly far upfield for a σ-bound aldehyde.[1] Yet, this upfield shift is a spectral property that is typical for σ-bound aldehyde complexes of pyrazolylborate molybdenum and tungsten complexes (vide infra). Tungsten coupling (^{183}W 14%, I = 1/2) to the aldehydic proton in the tungsten complexes reported in this work was not detected, suggesting *E*-conformational preferences about the C=O unit in our system.[17]

Ketones are σ-bound to Tp tungsten fragment **7** and have metal C≡O absorbances at approximately 1940 cm^{-1}.[14a] In contrast, the metal C≡O absorbances of aldehyde complexes **7a** and **7b** with the Tp tungsten fragment appear almost 100 cm^{-1} higher at 2042 and 2043 cm^{-1}, respectively (Table 1). Furthermore, both the aldehydic proton (C*H*O) in ^{1}H NMR and the aldehyde carbonyl carbon (*C*=O) in ^{13}C NMR are shifted significantly upfield relative to similar resonances of the Tp′ tungsten σ-complexes **5a** and **5b** and relative to free aldehydes. These spectral data indicate π-binding of saturated aldehydes to the Tp tungsten fragment **7**. The π-complexes **7a** and **7b** are amber in solution and are less soluble than comparable σ-complexes in methylene chloride.[18]

Several salient features in the ^{1}H and ^{13}C NMR spectra of aldehyde complexes of the Tp tungsten fragment **7** indicate the presence of a π-bound aldehyde ligand. (1) Since both substituents of the π-bound aldehyde are held in close proximity to the metal center, alkyne rotation is inhibited and the 2-butyne methyl substituents (≡C*Me*) appear as sharp resonances in the ^{1}H NMR spectra. In contrast, the alkyne methyl resonances in σ-bound ketone complexes of the Tp tungsten fragment **7** are broad.[14a] (2) Although alkyne rotation is inhibited in **7a** and **7b**, the alkyne carbons (*C*≡*C*) are broad in the ^{13}C NMR spectra. Furthermore, a downfield pyrazole carbon is broadened considerably relative to the other Tp pyrazole carbons. (3) While one alkyne carbon (≡*C*) resonates in the range expected for a four-electron-donating alkyne ligand (ca. 200 ppm),[19] the other alkyne carbon resonates at approximately 175 ppm, a shift that lies between four-electron- and three-electron-donating alkyne ligands. Normally, decreased alkyne donation reflects competitive donation between the alkyne $\pi_\perp$ and an ancillary metal ligand into the metal's single empty dπ-orbital.[14,20] Since a π-bound aldehyde ligand cannot competitively donate in this manner, we attribute the alkyne shift anomaly to a steric phenomenon in π-complexes, which may cause the alkyne to be less tightly bound to the metal center (vide infra). (4) The carbon of the metal *C*≡O in the ^{13}C NMR spectrum of **7a** is coupled to the aldehydic proton and appears as a doublet ($^3J_{CH}$ = 5 Hz) in ^{1}H-coupled ^{13}C NMR spectra. The aldehyde carbonyl resonance (*C*=O) in ^{13}C NMR also shows coupling to the aldehydic proton, and the coupling constant ($^1J_{CH}$ = 180 Hz) is the same in both σ- and π-aldehyde complexes of **5**−**8**.

A unique spectral feature of the π-bound acetaldehyde complex **7a** of the Tp tungsten fragment is the long-range coupling of the aldehydic proton to the alkyne methyl resonances in ^{1}H NMR.[21] The alkyne methyl protons resonate as two doublets at 3.31 and 2.79 ppm ($^5J_{HH}$ = 0.6 Hz). This unique coupling is likely due to reduced C=O slippage of the acetaldehyde ligand. Generally, the degree to which the carbon of the aldehyde C=O bond is slipped from the metal center decreases as the π-acidity of the aldehyde increases.[9d] Reduced C=O slippage would be expected in the π-acidic acetaldehyde ligand, encouraging coupling between the aldehyde and the alkyne methyl protons in **7a**.

Four diastereomeric aldehyde orientations are possible for π-bound complexes in the Tp tungsten complexes (**7**). These isomers differ in the C=O facial binding of the aldehyde and in the orientation of the aldehyde substituents relative to the metal center (Figure 2). High isomer selectivity is expected for π-complexes of Tp tungsten fragment **7**. Conformers **II** and **IV** are disfavored because the alkyl substituent of the aldehyde is oriented toward the sterically demanding Tp ligand. Conformations **I** and **III** differ in the orientation of the aldehyde oxygen relative to the metal C≡O.[22] Conformer **III** is disfavored because the pyrazole ring of N$_1$ is directed toward the alkyl substituent of

---

[17] The *E*-isomer has the aldehydic proton and the metal fragment *syn* to the C=O unit. Coupling between tungsten and the aldehydic proton can be utilized to assess *E*/*Z*-conformational preferences about the C=O unit in tungsten aldehyde complexes. Observable ^{183}W satellites indicate a larger average $^3J_{WH}$ value and a higher population of the *Z*-isomer. See ref 12.

[18] π/σ solubility differences have also been observed in the [CpRe(NO)(PPh$_3$)]$^+$ system. See ref 9c.

[19] Templeton, J. L. *Adv. Organomet. Chem.* **1989**, *29*, 1.

[20] Francisco, L. W.; White, P. S.; Templeton, J. L. *Organometallics* **1997**, *16*, 2547.

[21] Long-range coupling between bound aldehydes and ancillary ligands has been observed in other complexes. See: Yao, W.; Crabtree, R. H. *Inorg. Chem.* **1996**, *35*, 3007.

[22] Isomers **I** and **III** likely equilibrate rapidly via interconversion through a σ-intermediate. However, due to the low solubility of complexes **7a** and **7b** in CD$_2$Cl$_2$ and to the propensity of organic carbonyl ligands to undergo displacement by high-polarity solvents, we were unable to perform low-temperature NMR experiments to probe for the presence of these isomers. See: Méndez, N. Q.; Mayne, C. L.; Gladysz, J. A. *Angew. Chem., Int. Ed. Engl.* **1990**, *29*, 1475.

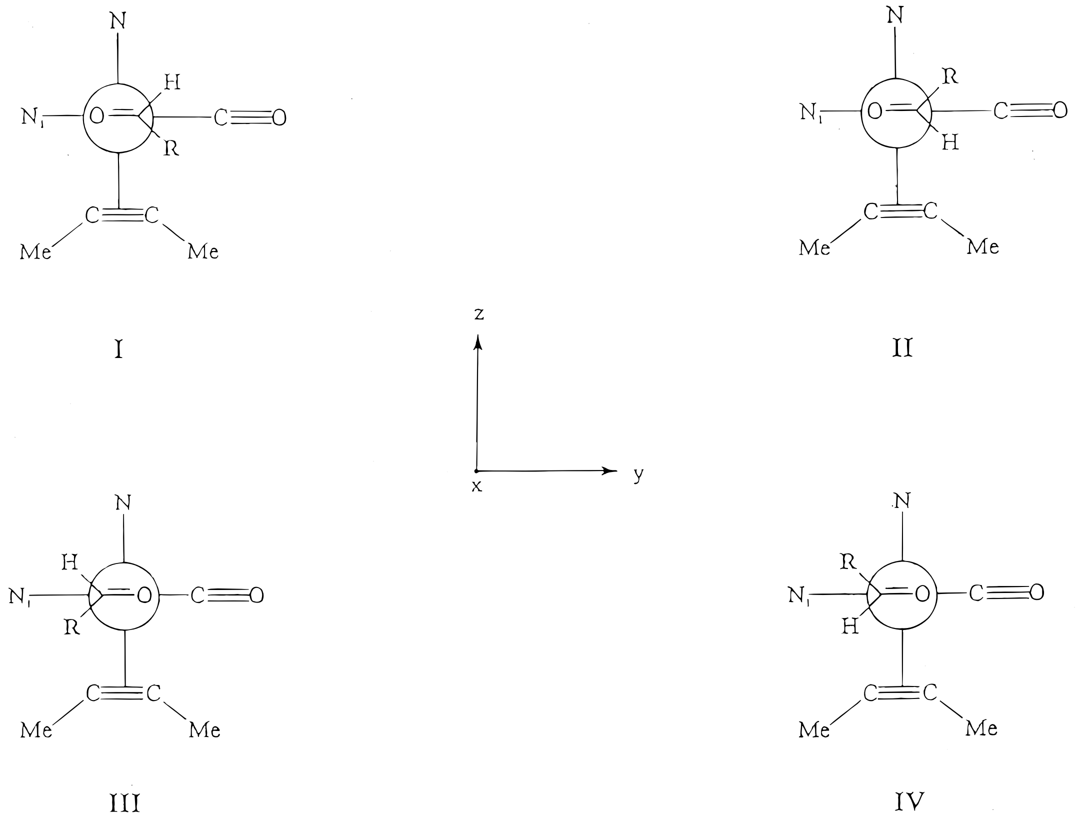

Figure 2. π-Stereoisomers of the [TpW(CO)(MeC≡CMe)]$^+$ fragment **7**.

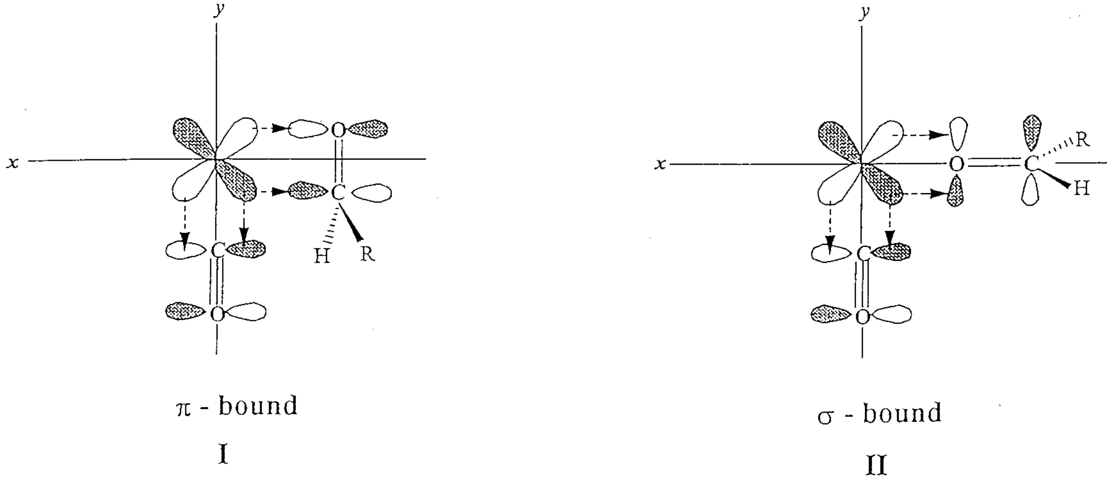

Figure 3. Orbital interactions in π- and σ-complexes of the [TpW(CO)(MeC≡CMe)]$^+$ fragment **7**.

the aldehyde, as seen in the structurally characterized *p*-anisaldehyde π-complex [TpW(CO)(MeC≡CMe)(η^2-*p*-O=CHC$_6$H$_4$OMe)][BAr′$_4$] (**7i**).[23]

Pivaldehyde is bulky and less π-acidic than acetaldehyde and propionaldehyde, and it is predominantly σ-bound in the Tp tungsten complex **7c**. Two C≡O absorbances are observed in the ambient temperature IR at 2046 and 1954 cm^{-1}, corresponding to π- and σ-isomers in a 11:89 ratio, respectively. Due to the spectroscopic time scale in ^{1}H NMR, only the averaged resonances of the rapidly equilibrating π- and σ-isomers are observed at room temperature for the characteristic aldehyde (C*H*O) resonance. Exchange of free and bound pivaldehyde was not observed in ^{1}H NMR upon addition of pivaldehyde to an NMR sample of **7c**, indicating that the $\pi \rightleftharpoons \sigma$ equilibration is intramolecular. The aldehyde *C*=O resonance in ^{13}C NMR is located at 210.9 ppm at −20 °C and is representative of a σ-complex. Complex **7c** is much less stable than the π-bound complexes **7a** and **7b** and decomposes quickly both in solution and in the solid state.

Metal C≡O IR absorbances of π- and σ-isomers of the Tp tungsten pivaldehyde complex **7c** differ by almost 100 cm^{-1}. Substantial competitive back-bonding from the metal d$_{xy}$-orbital to the metal C≡O π^*-orbital and to the aldehyde C=O π^*-orbital exists in π-complexes (**I** in Figure 3). With back-bonding to the aldehyde C=O π^*-orbital diminished in the σ-complex (**II** in Figure 3), the d$_{xy}$ electron density is directed into the π^*-orbital of the metal C≡O, lowering the metal C≡O absorbance

---

[23] Schuster, D. M.; White, P. S.; Templeton, J. I. *Organometallics* **1996**, *15*, 5467.

Table 2. Selected Data for α,β-Unsaturated Aldehyde Complexes [{Tp}M(CO)(R′C≡CMe)(O=CHR)][BAr′$_4$] (See Chart 2)

compound	R	mode (π/σ)[a]	IR, ν(C≡O) (cm^{-1}, CH$_2$Cl$_2$)	^{1}H NMR O=C*H*R (ppm)[b]	^{13}C NMR O=*C*HR (ppm)[b]
acrolein	−CH=CH$_2$			9.55	194.4
5d (Tp′W)	−CH=CH$_2$	σ	1942	7.53	198.4
6a (Tp′Mo)	−CH=CH$_2$	σ	1961	8.06	203.1
7d (TpW)	−CH=CH$_2$	π	2044	6.09	100.1
8a (TpMo)	−CH=CH$_2$	σ	1971	8.26	202.2
trans-crotonaldehyde	−CH=CHMe			9.47	193.8
5e (Tp′W)	−CH=CHMe	σ	1936	7.49	198.8
6b (Tp′Mo)	−CH=CHMe	σ	1957	7.93	201.8
7e (TpW)	−CH=CHMe	π/σ (55:45)	2033/1950	6.56	127.3
8b (TpMo)	−CH=CHMe	σ	1969	8.14	202.1
methacrolein	−C(Me)=CH$_2$			9.50	193.7
5f (Tp′W)	−C(Me)=CH$_2$	σ	1940	7.49	200.2
6c (Tp′Mo)	−C(Me)=CH$_2$	σ	1959	7.96	203.6
7f (TpW)	−C(Me)=CH$_2$	π/σ (86:14)	2041/1956	6.42	108.1
8c (TpMo)	−C(Me)=CH$_2$	σ	1972	8.21	203.9

[a] IR detection limit: 3%. [b] In CD$_2$Cl$_2$.

approximately 100 cm^{-1} relative to similar absorbances in π-complexes.

α,β-Unsaturated Aldehyde Complexes. The α,β-unsaturated aldehydes are σ- or π-bound to **5**, **6**, **7**, and **8** through the aldehyde C=O. Coordination of the olefinic double bond is incompatible with ^{1}H and ^{13}C NMR chemical shifts. At both ambient and low temperatures, α,β-unsaturated aldehydes are σ-bound to the Tp molybdenum fragment **8** and to the Tp′ tungsten and molybdenum fragments **5** and **6**. Analogous Tp tungsten complexes (**7**) exhibit both σ- and π-modes of coordination, depending on the nature of the aldehyde (Table 2). Acrolein is π-bound in complex **7d**, and *trans*-crotonaldehyde and methacrolein exhibit varying degrees of π/σ equilibration in complexes **7e** and **7f**, respectively. The π/σ ratios in the complexes conform to the relative carbonyl oxygen basicity and the π-acidity of the aldehyde. The aldehyde carbonyl resonance (*C*=O) in the ^{13}C NMR spectrum of the Tp tungsten *trans*-crotonaldehyde complex **7e** at 127.3 ppm is broad, and the chemical shift is between the shifts of pure σ- and π-isomers. At −60 °C, the *C*=O resonance of **7e** disappeared into the baseline, and it reappeared at −80 °C as a broad signal near 100 ppm, which sharpened as the temperature was lowered to −95 °C. The *C*=O resonance at 99.2 ppm at −95 °C is typical for a predominantly π-bound *trans*-crotonaldehyde complex. Signals for the corresponding decoalesced σ-isomer were not detected because the π/σ isomer ratio increases at lower temperatures, as determined by low-temperature IR spectroscopy (24 °C = 55:45; −7 °C = 68:32; −38 °C = 74:26).[9c,24]

The Tp′ complexes **5** and **6** are more electron-rich at the metal center and their metal C≡O IR absorbances are lower than the corresponding Tp complexes **7** and **8** (Table 2). Similarly, the more electron-rich tungsten complexes **5** and **7** have lower metal C≡O IR absorbances than the corresponding molybdenum complexes **6** and **8**.

Although the more electron-rich Tp′ complexes are more suited for back-bonding in π-complexation, the α,β-unsaturated aldehydes are σ-bound in the sterically demanding Tp′ tungsten and molybdenum complexes **5** and **6** (Table 2). The aldehyde C=O absorbance in the IR spectrum of the σ-bound *trans*-crotonaldehyde complexes **5e**, **6b**, and **8b** is approximately 75 cm^{-1} lower than the stretching frequency of free *trans*-crotonaldehyde (1703 cm^{-1}).

The vicinal $^3J_{\mathrm{HH}}$ couplings of 7−9 Hz between the α-proton (O=CHC*H*=) and the aldehydic proton (C*H*O) in σ-bound α,β-unsaturated complexes **5d**−**f**, **6a**−**c**, and **8a**−**c** are indicative of *s-trans* conformations for the coordinated enone in these complexes.[25,26]

X-ray Structure of [Tp′W(CO)(PhC≡CMe)(η^1-O=CHCH=CHMe)][BAr′$_4$] (5e). An ORTEP diagram of **5e** is shown in Figure 4. Crystallographic data and selected bond distances and angles are given in Tables 3 and 4, respectively. The *trans*-crotonaldehyde ligand is σ-bound to the metal center and adopts an *s-trans* configuration. The bent M−O−C orientation is common in complexes in which the aldehyde is σ-bound to a transition metal Lewis acid.[27] The angle of complexation (W1−O2−C3 = 139.0(5)°) is often larger than expected for an sp^2-hybridized oxygen. **5e** adopts the sterically less demanding *E*-conformation about the C=O bond. The tungsten metal is bent out of the O2−C3−C4−C5 plane by 16°. Slight bending of the metal toward the carbonyl π-orbital is common in transition metal complexes.[2a] The W1−O2 bond length of 2.069(4) Å is similar to W−O bond lengths in other structurally characterized tungsten α,β-unsaturated enone complexes.[28] The alkyne phenyl substituent is aligned with two of the pyrazole rings of the Tp′ ligand for optimum ring interactions. The aldehydic proton H3 is shielded by the pyrazole rings, which explains the unusual

---

[24] A custom-made variable-temperature stop/flow IR cell designed by Dr. S. A. Evans, Jr., of the University of North Carolina at Chapel Hill, for use with a Mattson Galaxy 5000 FTIR was employed.

[25] Coupling between the α-proton and aldehyde proton serves as a probe for *s-cis*/*s-trans* conformations in solution. A large $^3J_{\mathrm{HH}}$ value (approximately > 5 Hz) corresponds to a predominantly *s-trans* conformation. See: McNab, H. *J. Chem. Soc., Perkin Trans. 2* **1981**, 1283.

[26] The *s-trans* geometry of α,β-unsaturated aldehydes is often enhanced by coordination to a Lewis acid. See: Loncharich, R. J.; Schwartz, T. R.; Houk, K. N. *J. Am. Chem. Soc.* **1987**, *109*, 14.

[27] Theoretical investigations of aluminum and boron formaldehyde complexes identify this bent M−O−C structure as the ground-state geometry. See ref 2c.

[28] (a) Honeychuck, R. V.; Bonnesen, J. F.; Hersh, W. H. *J. Org. Chem.* **1987**, *52*, 5293. (b) Moriarty, R. E.; Ernst, R. D.; Bau, R. *J. Chem. Soc., Chem. Commun.* **1972**, 1242.

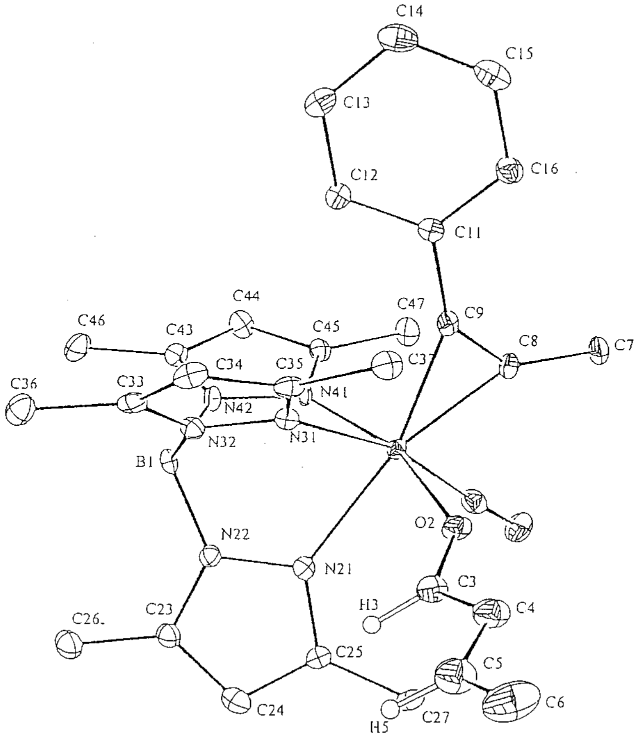

Figure 4. ORTEP diagram of [TpW(CO)(PhC≡CMe)(η^1-O=CHCH=CHMe)][BAr′$_4$] (**5e**).

Table 3. Crystallographic Data for [Tp′W(CO)(PhC≡CMe)(η^1-O=CHCH=CHMe)][BAr′$_4$] (5e)

molecular formula	$WC_{61}H_{48}F_{24}B_2N_6O_2$
fw, g/mol	1558.51
cryst dimens, mm	0.35 × 0.30 × 0.28
space group	$P\bar{1}$
collection temp	−170 °C
cell params	
a, Å	12.736(6)
b, Å	13.517(9)
c, Å	18.843(7)
V, A^3	3172(3)
Z	2
density calcd, g/cm^3	1.632
Collection and Refinement Parameters	
radiation (wavelength, Å)	Mo Kα (0.71073 Å)
monochromator	graphite
linear abs coeff, cm^{-1}	197.0
scan type	Ω
2θ limit	49.9°
h, k, l ranges	−15, 14; 0, 16; −22, 22
total no. of reflns	11245
data with $I > 2.5\sigma(I)$	8368
R	0.045
R_w	0.051
GOF	1.38
no. of params	866
max shift/σ	0.041

Table 4. Selected Bond Lengths (Å) and Angles (deg) for 5e

W(1)−C(1)	1.984(7)	C(1)−O(1)	1.150(8)
W(1)−O(2)	2.069(4)	O(2)−C(3)	1.232(8)
W(1)−C(8)	2.068(6)	C(3)−C(4)	1.423(10)
W(1)−C(9)	2.034(7)	C(4)−C(5)	1.328(11)
W(1)−N(21)	2.223(5)	C(5)−C(6)	1.489(11)
W(1)−N(31)	2.229(5)	C(7)−C(8)	1.489(9)
W(1)−N(41)	2.141(5)	C(8)−C(9)	1.330(9)
		C(9)−C(11)	1.449(9)
W(1)−C(1)−O(1)	176.8(6)	C(4)−C(5)−C(6)	125.4(8)
W(1)−O(2)−C(3)	139.0(5)	W(1)−C(8)−C(7)	149.5(5)
O(2)−C(3)−C(4)	122.9(7)	C(7)−C(8)−C(9)	140.8(6)
C(3)−C(4)−C(5)	121.5(7)	C(8)−C(9)−C(11)	139.7(6)

upfield shift of the aldehydic proton in ^{1}H NMR in σ-bound aldehyde complexes.[29]

Aromatic Aldehyde Complexes. Aromatic aldehydes are σ-bound to both the Tp′ tungsten **5** and Tp molybdenum **8** fragments and π- or σ-bound to the Tp tungsten fragment **7**, as determined by IR and ^{1}H and ^{13}C NMR (Table 5). *p*-Tolualdehyde and benzaldehyde are each π-bound to the Tp tungsten fragments (**7g** and **7h**), while *p*-anisaldehyde rapidly equilibrates between π- and σ-modes of coordination in the Tp tungsten complex **7i**. Generally, the *ortho* and *meta* aryl carbon resonances in the ^{13}C NMR spectra of the aromatic aldehyde complexes are broad, reflecting restricted rotation about the aryl−formyl bond due to π-delocalization from the electron-rich aryl group to the aldehyde functionality.[30]

A detailed description of the solution and solid-state structures of the Tp tungsten *p*-anisaldehyde complex **7i** and the Tp molybdenum *p*-anisaldehyde complex **8f** has been reported.[23] In solution, *p*-anisaldehyde is σ-bound in the Tp molybdenum complex **8f**, and in the tungsten complex **7i** it isomerizes between π- and σ-modes (Table 5). The *p*-anisaldehyde C=O bond length of 1.237(7) Å in the solid-state structure of **8f** is similar to the length in other structurally characterized σ-bound *p*-anisaldehyde complexes.[3d,9c,31]

In contrast, *p*-anisaldehyde is π-coordinated in the analogous Tp tungsten complex **7i** in the solid state. Due to the significant metal dπ-to-aldehyde π^* back-bonding in π-complexes, the *p*-anisaldehyde C=O bond length (1.308(14) Å) is substantially longer than in the σ-complex **8f**. In the solid-state geometry of **7i**, the aryl ring of the *p*-anisaldehyde ligand is directed away from the bulky Tp ligand, conforming to the predicted π-diastereoselectivity (**I** in Figure 2). The C=O bond is slipped from the tungsten metal center, where the W−C length (2.268(11) Å) is longer than the W−O bond length (1.974(6) Å). The W−C$_{\text{alkyne}}$ bond lengths in **7i** (2.049(11) and 2.090(10) Å) are longer than expected for a four-electron-donating alkyne (ca. 2.00 Å)[19] and suggest a less tightly bound alkyne in π-complexes. This is likely due to the sterically demanding environment in π-complexes, and it explains the unusual upfield shift of one of the alkyne carbons (≡*C*) in ^{13}C NMR spectra of π-complexes.

Variable-Temperature FTIR Experiment. The *p*-anisaldehyde carbonyl carbon (*C*=O) of **7i** was broadened into the baseline at ambient temperature in ^{13}C NMR, due to the dynamic π/σ equilibrium. The decoa-

---

(29) Acidity scales derived from NMR chemical shift differences, such as Childs' scale based on the degree of downfield shifting of the β-proton of bound versus free *trans*-crotonaldehyde, can be used to assess relative Lewis acidity. These scales are not applicable to the Lewis acids in this paper because the β-proton H5 is also shielded and is shifted upfield relative to the β-proton of free *trans*-crotonaldehyde. See: Childs, R. F.; Mulholland, D. L.; Nixon, A. *Can. J. Chem.* **1982**, *60*, 801.

(30) For comparison of internal rotation about the C−C bond in free versus Lewis acid-coordinated aromatic aldehydes, see: (a) Grinvald, A.; Rabinovitz, M. *J. Chem. Soc., Perkin Trans. 2* **1974**, 94. (b) Greenvald, A.; Rabinovitz, M. *J. Chem. Soc., Chem. Commun.* **1969**, 642. (c) Anet, F. A. L.; Ahmad, M. *J. Am. Chem. Soc.* **1964**, *86*, 119.

(31) Bochmann, M.; Webb, K. J.; Hursthouse, M. B.; Mazid, M. *J. Chem. Soc., Chem. Commun.* **1991**, 1735.

Table 5. Selected Data for Aromatic Aldehyde Complexes [{Tp}M(CO)(R′C≡CMe)(O=CHR)][BAr′$_4$] (See Chart 2)

compound	R	mode (π/σ)[a]	IR, ν(C≡O) (cm^{-1}, CH$_2$Cl$_2$)	^{1}H NMR O=C*H*R (ppm)[b]	^{13}C NMR O=*C*HR (ppm)[b]
benzaldehyde	$-C_6H_5$			10.01	192.0
5g[c] (Tp′W)	$-C_6H_5$	σ	1939	7.83	195.3
7g (TpW)	$-C_6H_5$	π	2040	6.77	98.8
8d (TpMo)	$-C_6H_5$	σ	1977	8.53	199.1
p-tolualdehyde	4-C_6H_4Me			9.95	190.8
5h (Tp′W)	4-C_6H_4Me	σ	1937	7.76	195.6
7h (TpW)	4-C_6H_4Me	π	2035	6.85	103.7
8e (TpMo)	4-C_6H_4Me	σ	1970	8.45	199.2
p-anisaldehyde	4-C_6H_4OMe			9.86	189.6
5i (Tp′W)	4-C_6H_4OMe	σ	1932	7.68	193.8
7i (TpW)	4-C_6H_4OMe	π/σ (53:47)	2033/1944	7.15	97.1[d]
8f (TpMo)	4-C_6H_4OMe	σ	1968	8.30	197.2

[a] IR detection limit: 3%. [b] In CD$_2$Cl$_2$. [c] Unpublished data. See ref 14b for the [BF$_4$]$^-$ analogue. [d] ^{13}C NMR spectrum taken at −95 °C.

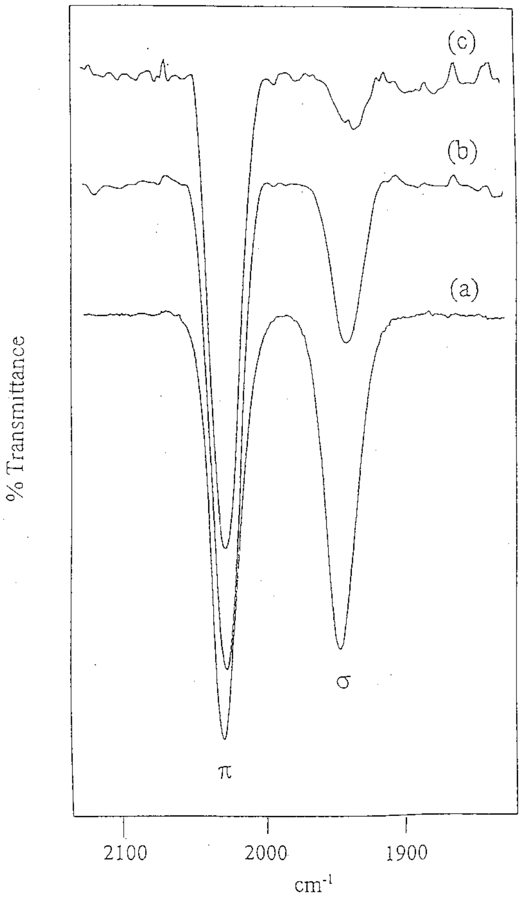

Figure 5. Variable-temperature IR spectra of [TpW(CO)(MeC≡CMe)(η^1/η^2-*p*-O=CHC$_6$H$_4$OMe)][BAr′$_4$] (**7i**): (a) 21 °C, (b) −42 °C, (c) −78 °C.

lesced *C*=O resonance of the π-isomer of **7i** can be detected in ^{13}C NMR at − 80 °C. However, the corresponding decoalesced *C*=O resonance of the σ-isomer was not detected in ^{13}C NMR spectra of **7i** to −130 °C[32] because the π/σ ratio increases as the temperature is lowered. The 53:47 π/σ ratio at 21 °C increases to 94:6 at −78 °C, as observed in variable-temperature FTIR spectra. (Figure 5, Table 6). Therefore, detection of the *C*=O resonance of the minor decoalesced σ-isomer of **7i** in low-temperature ^{13}C NMR is not expected.

Table 6. Variable-Temperature IR Data for [TpW(CO)(MeC≡CMe)(η^1/η^2-*p*-O=CHC$_6$H$_4$OMe)][BAr′$_4$] (7i)

temp (°C)	π/σ	$\Delta G°$ (kcal/mol)[a]
21	53:47	−0.08
−42	74:26	−0.68
−78	94:6	−1.00

[a] For $\sigma \rightarrow \pi$.

Summary

The series of closely related Tp′ and Tp molybdenum and tungsten Lewis acids presented here illustrates several factors that influence the mode of aldehyde coordination: the aldehyde, the metal, and the steric imposition of the metal's ancillary ligands. Aldehydes are σ-bound in the electron-rich yet sterically demanding Tp′ molybdenum and tungsten fragments **5** and **6**. In contrast, the Tp tungsten fragment **7** has a more open coordination environment and exhibits both σ- and π-modes of aldehyde coordination depending on the nature of the aldehyde: saturated aldehydes are π-bound; the bulky pivaldehyde ligand is predominantly σ-bound; and aromatic and α,β-unsaturated aldehydes exhibit π/σ-modes of coordination, depending on the carbonyl oxygen basicity and π-acidity of these aldehydes. In clear contrast to the Tp tungsten fragment **7**, aldehydes are exclusively σ-bound to the less electron-rich Tp molybdenum fragment **8**, demonstrating the effect the metal has on the aldehyde coordination mode.

Experimental Section

Reactions were carried out under a purified nitrogen atmosphere using standard Schlenk techniques. Hexane was distilled from sodium benzophenone ketyl; methylene chloride was distilled from phosphorus pentoxide. The aldehydes were dried over 4 Å molecular sieves prior to use. Acetaldehyde and benzaldehyde were distilled before drying over 4 Å molecular sieves. CD$_2$Cl$_2$ was degassed and dried over 4 Å molecular sieves. HBAr′$_4$·2OEt$_2$ (BAr′$_4$ = tetrakis[3,5-bis(trifluoromethyl)phenyl]borate) was prepared according to the literature.[15b] Complexes **1**−**4**,[14a] **7i** and **8f**,[23] and **5g** and **5c**[14b] were synthesized according to published procedures.

^{1}H and ^{13}C NMR spectra were recorded on a Bruker AC 200 (200 MHz), a Bruker WM 250 (250 MHz), or a Varian XL 400 (400 MHz) spectrometer. Infrared spectra at ambient temperature were collected on a Mattson Polaris FTIR spectrometer. Variable-temperature IR spectra for complexes **7e** and **7i** were collected on a Mattson Galaxy 5000 FTIR spectrometer.[24]

---

[32] Coalescence temperatures below −95 °C were obtained in CDFCl$_2$. See: Siegel, J. S.; Anet, F. A. L. *J. Org. Chem.* **1988**, *53*, 2629.

Elemental analyses were performed by Atlantic Microlab of Norcross, GA.

Variable-Temperature Infrared Measurements. To confirm the Beer's law relationship for π- and σ-complexes, a CH_2Cl_2 solution was prepared that was 0.07 M in both the σ-acetone complex [TpW(CO)(MeC≡CMe)(η^1-O=CMe_2)][BAr′$_4$][14a] and the π-acetaldehyde complex [TpW(CO)(MeC≡CMe)(η^2-O=CHMe)][BAr′$_4$] (**7a**). The areas of the peaks (absorbance mode: cut/weigh) were within 0.1% of a 1:1 ratio. The π/σ ratios for complex **7i** were then calculated from the C≡O absorbances of the π- and σ-isomers.

NMR Data. Full ^1H and ^{13}C NMR data are reported only for complex **5a** and **7a** as representative data. ^1H and ^{13}C NMR data for the [BAr′$_4$]$^-$ counterion are reported separately for simplicity. Complete NMR data are available for all complexes in the Supporting Information.

Representative [BAr′$_4$]$^-$: ^1H NMR (CD_2Cl_2) δ 7.77 (br, 8 H, *o*-Ar′), 7.60 (br, 4 H, *p*-Ar′); $^{13}C\{H\}$ NMR (CD_2Cl_2) δ 162.2 (q, $^1J_{BC}$ = 50 Hz, *ipso*-C), 135.3 (*o*-C), 129.4 (qq, $^2J_{CF}$ = 30 Hz, $^4J_{CF}$ = 5 Hz, *m*-C), 125.1 (q, $^1J_{CF}$ = 270 Hz, CF_3), 117.9 (m, *p*-C).

Synthesis of [{Tp}M(CO)(RC≡CR′)(aldehyde)][BAr′$_4$] Complexes. In a typical experiment, 0.10 g of {Tp}M(CO)(RC≡CR′)Me (**1**–**4**) in CH_2Cl_2 (10 mL) was cooled to −78 °C. In a separate Schlenk flask, a CH_2Cl_2 solution (5 mL) of HBAr′$_4$·2OEt_2 (1 equiv) was cooled to −78 °C. The two solutions were mixed at −78 °C, aldehyde (0.8 mL) was added, and the reaction mixture was allowed to warm to ambient temperature. The solution was stirred for 5 min before the solvent was removed in vacuo. The residue was triturated with hexanes and recrystallized from layered CH_2Cl_2/hot hexanes.

[Tp′W(CO)(PhC≡CMe)(η^1-O=CHMe)][BAr′$_4$] (5a): green crystals; 69% yield; IR (CH_2Cl_2) 1939 ($\nu_{C\equiv O}$) cm^{-1}; ^1H NMR (CD_2Cl_2) δ 7.90 (q, 1 H, $^3J_{HH}$ = 4.0 Hz, C*H*O), 7.36−7.25, 6.81−6.70 (each a m, 3:2 H, ≡C*Ph*), 6.09, 5.87, 5.80 (each a s, each 1 H, Tp′−*H*), 3.92 (s, 3 H, ≡C*Me*), 2.59 (d, 3 H, $^3J_{HH}$ = 4.0 Hz, O=CH*Me*), 2.54, 2.52, 2.43, 1.34, 1.13 (each a s, 3:3:6:3:3 H, Tp′−*Me*); $^{13}C\{H\}$ NMR (CD_2Cl_2) δ 224.0 (*C*≡O), 210.4 (*C*=O), 208.6 (≡*C*Ph), 207.3 (≡*C*Me), 153.1, 151.8, 151.5, 148.9, 148.4, 146.7 (Tp′−*C*−Me), 135.6 (*ipso* of ≡C*Ph*), 131.1, 130.0, 129.3 (*p*, *m*, *o* of ≡C*Ph*), 109.4, 109.4, 108.5 (Tp′−*C*−H), 30.1 (O=CH*Me*), 23.2 (≡C*Me*), 16.1, 15.3, 13.5, 13.1, 12.9, 12.6 (Tp′−*Me*). Anal. Calcd based on $WC_{59}H_{46}N_6B_2O_2F_{24}\cdot 0.5CH_2Cl_2$ (CH_2Cl_2 determined by ^1H NMR): C, 45.37; H, 3.01; N, 5.34. Found: C, 45.38; H, 3.14; N, 5.44.

[Tp′W(CO)(PhC≡CMe)(η^1-O=CHEt)][BAr′$_4$] (5b): green crystals; 78% yield; IR (CH_2Cl_2) 1939 ($\nu_{C\equiv O}$) cm^{-1}; ^1H NMR (CD_2Cl_2) δ 7.90 (t, 1 H, $^3J_{HH}$ = 2.3 Hz, C*H*O), 2.91 (m, 2 H, O=CH(CH_2CH_3)), 0.97 (t, 3 H, $^3J_{HH}$ = 7.3 Hz, O=CH(CH_2CH_3)); $^{13}C\{H\}$ NMR (CD_2Cl_2) δ 214.9 (*C*=O), 37.5 (O=CH(*C*H_2CH_3)), 6.7 (O=CH(CH_2*C*H_3)). Anal. Calcd: C, 46.60; H, 3.13; N, 5.43. Found: C, 46.57; H, 3.21; N, 5.43.

[Tp′W(CO)(PhC≡CMe)(η^1-O=CHCH=CH_2)][BAr′$_4$] (5d): magenta crystals; 85% yield; IR (CH_2Cl_2) 1942 ($\nu_{C\equiv O}$) cm^{-1}; ^1H NMR (CD_2Cl_2) δ 67.53 (d, 1 H, $^3J_{HH}$ = 8.8 Hz, C*H*O), 6.47 (ddd, 1 H, $^3J_{HH}$ = 17.2, 10.0, 8.8 Hz, O=CHC*H*=), 6.09 (d, 1 H, $^3J_{HH}$ = 10.0 Hz, =C*H*(H)), 5.92 (d, 1 H, $^3J_{HH}$ = 17.2 Hz, =CH(*H*)); $^{13}C\{H\}$ NMR (CD_2Cl_2) δ 198.4 (*C*=O); 143.6 (=*C*H_2), 134.6 (O=HC*C*H=). Anal. Calcd based on $WC_{60}H_{46}N_6B_2O_2F_{24}\cdot 0.5CH_2Cl_2$ (CH_2Cl_2 determined by ^1H NMR): C, 45.79; H, 2.99; N, 5.30. Found: C, 45.70; H, 3.15; N, 5.35.

[Tp′W(CO)(PhC≡CMe)(η^1-O=CHCH=CHMe)][BAr′$_4$] (5e): red crystals; 85% yield; IR (CH_2Cl_2): 1936 ($\nu_{C\equiv O}$) cm^{-1}, 1626 ($\nu_{C=O}$) cm^{-1}; ^1H NMR (CD_2Cl_2) δ 7.49 (d, 1 H, $^3J_{HH}$ = 9.2 Hz, C*H*O), 6.70 (dq, 1 H, $^3J_{HH}$ = 15.2, 7.2 Hz, =C*H*Me), 6.27 (ddq, 1 H, J_{HH} = 15.2, 9.2, 1.6 Hz, O=CHC*H*=), 2.21 (dd, 3 H, J_{HH} = 7.2, 1.6 Hz, =CH*Me*); $^{13}C\{H\}$ NMR (CD_2Cl_2) δ 198.8 (*C*=O), 164.4 (=*C*HMe), 131.9 (O=CH*C*H=), 19.9 (=CH*Me*). Anal. Calcd.: C, 47.00; H, 3.10; N, 5.39. Found: C, 47.10; H, 3.20; N, 5.33.

[Tp′W(CO)(PhC≡CMe)(η^1-O=CHC(Me)=CH_2)][BAr′$_4$] (5f): purple powder; 68% yield; IR (CH_2Cl_2) 1940 ($\nu_{C\equiv O}$) cm^{-1}; ^1H NMR (CD_2Cl_2) δ 7.49 (s, 1 H, C*H*O), 5.97, 5.68 (each a s, each 1 H, =CH_2), 1.62 (s, 3 H, O=CHC(*Me*)=); $^{13}C\{H\}$ NMR (CD_2Cl_2) δ 200.2 (*C*=O), 143.8 (O=CH*C*(Me)=), 142.4 (=*C*H_2), 14.2 (O=CHC(*Me*)=). Anal. Calcd: C, 47.00; H, 3.10; N, 5.39. Found: C, 47.12; H, 3.18; N, 5.49.

[Tp′W(CO)(PhC≡CMe)(η^1-*p*-O=CHC_6H_4Me)][BAr′$_4$] (5h): magenta crystals; 68% yield; IR (CH_2Cl_2) 1937 ($\nu_{C\equiv O}$) cm^{-1}; ^1H NMR (CD_2Cl_2) δ 7.76 (s, 1 H, C*H*O), 7.33 (br s, 4 H, C_6H_4), 2.52 (s, 3 H, C_6H_4-*Me*); $^{13}C\{H\}$ NMR (CD_2Cl_2) δ 195.6 (*C*=O), 152.0 (*ipso* of C_6H_4), 132.2 (br, C_6H_4), 131.0 (*C*-Me of C_6H_4), 22.3 (C_6H_4-*Me*). Anal. Calcd: C, 48.53; H, 3.13; N, 5.22. Found: C, 48.55; H, 3.15; N, 5.26.

[Tp′W(CO)(PhC≡CMe)(η^1-*p*-O=CHC_6H_4OMe)][BAr′$_4$] (5i): red crystals; 83% yield; IR (CH_2Cl_2) 1932 ($\nu_{C\equiv O}$) cm^{-1}; ^1H NMR (CD_2Cl_2) δ 7.68 (s, 1 H, C*H*O), 7.42, 6.97 (each a br d, each 2 H, J_{HH} = 8.4 Hz each, C_6H_4), 3.89 (s, 3 H, *OMe*); $^{13}C\{H\}$ NMR (CD_2Cl_2, −80 °C) δ 192.2 (*C*=O), 167.4 (*C*−OMe), 137.7, 131.5 (C_6H_4), 125.8 (*ipso* of C_6H_4), 116.4, 112.8 (C_6H_4), 56.1 (O*Me*). Anal. Calcd based on $WC_{65}H_{50}N_6B_2O_3F_{24}\cdot 0.5CH_2Cl_2$ (CH_2Cl_2 determined by ^1H NMR): C, 47.19; H, 3.08; N, 5.04. Found: C, 47.17; H, 3.20; N, 5.03.

[Tp′Mo(CO)(PhC≡CMe)(η^1-O=CHCH=CH_2)][BAr′$_4$] (6a): orange crystals; 64% yield; IR (CH_2Cl_2) 1961 ($\nu_{C\equiv O}$) cm^{-1}; ^1H NMR (CD_2Cl_2) δ 8.06 (m, 1 H, C*H*O), 6.49−6.01 (m, 3 H, O=CHC*H*=CH_2); $^{13}C\{H\}$ NMR (CD_2Cl_2) δ 203.1 (*C*=O), 145.5 (=*C*H_2), 135.4 (O=CH*C*H=). Anal. Calcd: C, 49.48; H, 3.18; N, 5.77. Found: C, 49.45; H, 3.32; N, 5.92.

[Tp′Mo(CO)(PhC≡CMe)(η^1-O=CHCH=CHMe)][BAr′$_4$] (6b): brown powder, green crystals; 64% yield; IR (CH_2Cl_2) 1957 ($\nu_{C\equiv O}$) cm^{-1}, 1628 ($\nu_{C=O}$) cm^{-1}; ^1H NMR (CD_2Cl_2) δ 7.93 (d, 1 H, $^3J_{HH}$ = 9.0 Hz, C*H*O), 6.91 (dq, 1 H, $^3J_{HH}$ = 15.4, 7.0 Hz, =C*H*Me), 6.23 (ddq, 1 H, J_{HH} = 15.4, 9.0, 1.4 Hz, O=CHC*H*=), 2.04 (dd, 3 H, J_{HH} = 7.0, 1.4 Hz, =CH*Me*); $^{13}C\{H\}$ NMR (CD_2Cl_2) δ 201.8 (*C*=O), 165.6 (=*C*HMe), 132.5 (O=CH*C*H=), 20.2 (=CH*Me*). Anal. Calcd: C, 49.82; H, 3.29; N, 5.71. Found: C, 49.75; H, 3.25; N, 5.77.

[Tp′Mo(CO)(PhC≡CMe)(η^1-O=CHC(Me)=CH_2)][BAr′$_4$] (6c): amber crystals; 66% yield; IR (CH_2Cl_2) 1959 ($\nu_{C\equiv O}$) cm^{-1}; ^1H NMR (CD_2Cl_2) δ 7.96 (s, 1 H, C*H*O), 6.26 (br q, 1 H, $^4J_{HH}$ = 1.4 Hz, =CH(*H*)), 5.91 (s, 1 H, =C*H*(H)), 1.69 (s, 3 H, O=CHC(*Me*)=); $^{13}C\{H\}$ NMR (CD_2Cl_2) δ 203.6 (*C*=O), 144.5, 143.5 (O=CH*C*(Me)=*C*H_2), 15.3, 15.1, 13.9, 13.2, 13.0, 12.9, 12.7 (Tp′−*Me*, O=CHC(*Me*)=). Anal. Calcd: C, 49.82; H, 3.29; N, 5.71. Found: C, 49.66; H, 3.27; N, 5.83.

[TpW(CO)(MeC≡CMe)(η^2-O=CHMe)][BAr′$_4$] (7a): yellow crystals; 88% yield; IR (CH_2Cl_2) 2042 ($\nu_{C\equiv O}$) cm^{-1}; ^1H NMR (CD_2Cl_2) δ 8.25 (d, 1 H, $^3J_{HH}$ = 2.2 Hz, 3,5-Tp *H*), 8.05 (dd, 1 H, $^3J_{HH}$ = 2.0 Hz, $^3J_{HH}$ = 0.8 Hz, 3,5-Tp *H*), 7.86 (m, 2 H, 3,5-Tp *H*), 7.77 (obscured by *o-Ar′*, 1 H, Tp *H*), 6.70 (m, 2 H, Tp *H*), 6.40, 6.24 (each a t, each 1 H, $^3J_{HH}$ = 2.4 Hz each, 4-Tp *H*), 5.93 (br q, 1 H, $^3J_{HH}$ = 4.4 Hz, O=C*H*Me), 3.31, 2.79 (each a d, each 3 H, $^5J_{HH}$ = 0.6 Hz each, *Me*C≡C*Me*), 2.39 (d, 3 H, $^3J_{HH}$ = 4.4 Hz, O=CH*Me*); $^{13}C\{H\}$ NMR (CD_2Cl_2) δ 207.0 (*C*≡O), 197.8, 173.5 (each br, Me*C*≡*C*Me), 144.6, 143.5 (Tp−*C*), 143.0 (br, Tp−*C*), 138.7, 137.9, 137.6, 108.5, 108.4, 108.3 (Tp−*C*), 98.4 (*C*=O), 22.4 (O=CH*Me*), 20.3, 18.1 (*Me*C≡C*Me*). Anal. Calcd based on $WC_{48}H_{32}N_6B_2O_2F_{24}\cdot 0.5CH_2Cl_2$ (CH_2Cl_2 determined by ^1H NMR): C, 40.77; H, 2.33; N, 5.88. Found: C, 40.54; H, 2.45; N, 5.84.

[TpW(CO)(MeC≡CMe)(η^2-O=CHEt)][BAr′$_4$] (7b): amber crystals; 76% yield; IR (CH_2Cl_2) 2043 ($\nu_{C\equiv O}$) cm^{-1}; ^1H NMR (CD_2Cl_2) δ 5.80 (m, 1 H, C*H*O), 2.63 (m, 1 H, O=CH(C*H*(H)Me)), 1.31 (m, 4H, O=CH(CH(*H*)*Me*)); $^{13}C\{H\}$ NMR (CD_2Cl_2) δ 103.8 (*C*=O), 30.5 (O=CH(*C*H_2Me)), 20.4, 18.0, 15.5 (*Me*C≡C*Me*, O=CH(CH_2*Me*)). Anal. Calcd based on $WC_{49}H_{34}N_6B_2O_2F_{24}\cdot CH_2Cl_2$ (CH_2Cl_2 determined by ^1H NMR): C, 40.43; H, 2.44; N, 5.66. Found: C, 40.85; H, 2.67; N, 5.83.

[TpW(CO)(MeC≡CMe)(η^1/η^2-O=CH^tBu)][BAr′$_4$] (7c). The product is stable below −20 °C for approximately 2 h: purple powder; 28% yield; IR (CH_2Cl_2) (11:89, π/σ), 2046/1954 ($\nu_{C\equiv O}$) cm^{-1}; ^{1}H NMR (CD_2Cl_2) δ 7.29 (s, 1 H, *CHO)*, 0.96 (s, 9 H, O=CH(C*Me*$_3$)); ^{13}C{H} NMR (CD_2Cl_2, −20 °C) δ 210.9 (*C*=O), 42.8 (O=CH(*C*Me$_3$)), 25.4 (O=CH(C*Me*$_3$)).

[TpW(CO)(MeC≡CMe)(η^2-O=CHCH=CH$_2$)][BAr′$_4$] (7d): amber crystals; 93% yield; IR (CH_2Cl_2) 2044 ($\nu_{C\equiv O}$) cm^{-1}; ^{1}H NMR (CD_2Cl_2) δ 6.09 (br d, 1 H, $^3J_{HH}$ = 7.3 Hz, C*H*O), 5.60 (d, 1 H, $^3J_{HH}$ = 17.5 Hz, =C*H*(H)), 5.44 (d, 1 H, $^3J_{HH}$ = 10.5 Hz, =CH(*H*)), 5.16 (ddm, 1 H, $^3J_{HH}$ = 17.5, 10.5 Hz, O=CHC*H*=); ^{13}C{H} NMR (CD_2Cl_2) δ 135.0 (=*C*H$_2$), 127.2 (O=CH*C*H=), 100.1 (br, *C*=O). Anal. Calcd based on $WC_{49}H_{32}N_6B_2O_2F_{24}\cdot 0.5CH_2Cl_2$ (CH_2Cl_2 determined by ^{1}H NMR): C, 41.27; H, 2.31; N, 5.83. Found: C, 41.29; H, 2.47; N, 5.78.

[TpW(CO)(MeC≡CMe)(η^1/η^2-O=CHCH=CHMe)][BAr′$_4$] (7e): dark orange crystals; 84% yield; IR (CH_2Cl_2) (55:45, π/σ), 2033/1950 ($\nu_{C\equiv O}$) cm^{-1}; ^{1}H NMR (CD_2Cl_2) δ 6.56 (d, 1 H, $^3J_{HH}$ = 8.3 Hz, C*H*O), 6.48 (dq, 1 H, $^3J_{HH}$ = 15.3, 7.0 Hz, =C*H*Me), 5.15 (ddq, 1 H, J_{HH} = 15.3, 8.3, 1.8 Hz, O=CHC*H*=), 2.35 (dd, 3 H, J_{HH} = 7.0, 1.8 Hz, =CH*Me*); ^{13}C{H} NMR (CD_2Cl_2) δ 148.1 (=*C*HMe), 129.2 (O=CH*C*H=), 127.3 (br, *C*=O), 18.5 (=CH*Me*). Anal. Calcd based on $WC_{50}H_{34}N_6B_2O_2F_{24}\cdot C_6H_{14}$ (hexane determined by ^{1}H NMR): C, 44.88; H, 3.23; N, 5.61. Found: C, 44.38; H, 3.14; N, 5.75.

[TpW(CO)(MeC≡CMe)(η^1/η^2-O=CHC(Me)=CH$_2$)][BAr′$_4$] (7f): dark orange powder, amber crystals; 71% yield; IR (CH_2Cl_2) (86:14, π/σ), 2041/1956 ($\nu_{C\equiv O}$) cm^{-1}; ^{1}H NMR (CD_2Cl_2) δ 6.42 (s, 1 H, C*HO*), 5.44, 5.24 (each a br s, each 1 H, =C*H*$_2$), 1.00 (s, 3 H, O=CHC(*Me*)=); ^{13}C(H) NMR(CD_2Cl_2) δ 141.0 (O=CH*C*(Me)=), 124.7 (br, =*C*H$_2$), 108.1 (br, *C*=O), 15.3 (O=CHC(*Me*)=). Anal. Calcd for $WC_{50}H_{34}N_6B_2O_2F_{24}\cdot 0.5CH_2Cl_2$ (CH_2Cl_2 determined by ^{1}H NMR): C, 41.69; H, 2.43; N, 5.78. Found: C, 41.79; H, 2.50; N, 5.76.

[TpW(CO)(MeC≡CMe)(η^2-O=CHPh)][BAr′$_4$] (7g): dark yellow crystals; 80% yield; IR (CH_2Cl_2) 2040 ($\nu_{C\equiv O}$) cm^{-1}; ^{1}H NMR (CD_2Cl_2) δ 7.60−7.28 (m, 5 H, O=CH*Ph*), 6.77 (s, 1 H, C*HO*); ^{13}C{H} NMR (CD_2Cl_2, −60 °C) δ 133.9 (*ipso* of Ph), 132.1, 129.0, 128.7, 128.5, 122.6 (*p, o, m* of Ph), 95.9 (*C*=O). Anal. Calcd based on $WC_{53}H_{34}N_6B_2O_2F_{24}\cdot 0.5CH_2Cl_2$ (CH_2Cl_2 determined by ^{1}H NMR): C, 43.10; H, 2.37; N, 5.64. Found: C, 42.73; H, 2.51; N, 5.74.

[TpW(CO)(MeC≡CMe)(η^2-*p*-O=CHC$_6$H$_4$Me)][BAr′$_4$] (7h): amber crystals; 79% yield; IR (CH_2Cl_2) 2035 ($\nu_{C\equiv O}$) cm^{-1}; ^{1}H NMR (CD_2Cl_2) δ 7.77 (obscured by *o*-Ar′, 2 H, C$_6$*H*$_4$), 7.29 (br d, 2 H, J_{HH} = 7.5 Hz, C$_6$*H*$_4$), 6.85 (s, 1 H, C*H*O), 2.55 (s, 3 H, C$_6$H$_4$−*Me*); ^{13}C{H} NMR (CD_2Cl_2, −80 °C) δ 142.7 (*C*−Me of C$_6$H$_4$), 130.3 (*ipso* of C$_6$H$_4$), 129.2, 128.9, 128.1, 122.2 (*o, m* of C$_6$H$_4$), 96.3 (*C*=O), 20.7, 17.8, 17.4 (*Me*C≡C*Me*, C$_6$H$_4$−*Me*). Anal. Calcd: C, 44.35; H, 2.48; N, 5.75. Found: C, 44.20; H, 2.50; N, 5.87.

[TpMo(CO)(MeC≡CMe)(η^1-O=CHCH=CH$_2$)][BAr′$_4$] (8a). Considerable decomposition accompanied the formation of **8a**: brown powder, green crystals; IR (CH_2Cl_2) 1971 ($\nu_{C\equiv O}$) cm^{-1}; ^{1}H NMR (CD_2Cl_2) δ 8.26 (d, 1 H, $^3J_{HH}$ = 7.8 Hz, C*H*O), 6.47−6.17 (m, 5 H, O=CHC*H*=C*H*$_2$, 2 Tp *H*); ^{13}C(H) NMR (CD_2Cl_2) δ 202.2 (*C*=O), 145.3 (=*C*H$_2$), 135.0 (O=CH*C*H=).

[TpMo(CO)(MeC≡CMe)(η^1-O=CHCH=CHMe)][BAr′$_4$] (8b): brown powder, green crystals; 85% yield; IR (CH_2Cl_2) 1969 ($\nu_{C\equiv O}$) cm^{-1}, 1628 ($\nu_{C=O}$) cm^{-1}; ^{1}H NMR (CD_2Cl_2) δ 8.14 (d, 1 H, $^3J_{HH}$ = 8.8 Hz, C*H*O), 6.95 (dq, $^3J_{HH}$ = 15.3, 7.0 Hz, =C*H*Me), 6.11 (ddq, 1 H, J_{HH} = 15.3, 8.8, 1.6 Hz, O=CHC*H*=), 2.09 (dd, 3 H, J_{HH} = 7.0, 1.6 Hz, =CH*Me*); ^{13}C{H} NMR (CD_2Cl_2) δ 202.1 (*C*=O), 165.8 (=*C*HMe), 131.9 (O=CH*C*H=), 20.2 (=CH*Me*). Anal. Calcd based on $MoC_{50}H_{34}N_6B_2O_2F_{24}\cdot 0.5C_6H_{14}$ (hexane determined by ^{1}H NMR): C, 46.55; H, 3.02; N, 6.14. Found: C, 46.18; H, 2.76; N, 5.74.

[TpMo(CO)(MeC≡CMe)(η^1-O=CHC(Me)=CH$_2$)][BAr′$_4$] (8c): green crystals; 74% yield; IR (CH_2Cl_2) 1972 ($\nu_{C\equiv O}$) cm^{-1}, 1586 ($\nu_{C=O}$) cm^{-1}; ^{1}HNMR (CD_2Cl_2) δ 8.21 (s, 1 H, C*H*O), 6.23 (br, 1 H, =CH(*H*)), 5.93 (s, 1 H, =C*H*(H)), 1.61 (s, 3 H, O=CHC(*Me*)=); ^{13}C{H} NMR (CD_2Cl_2) δ 203.9 (*C*=O), 144.4 (O=CH*C*(Me)=), 143.1 (=*C*H$_2$), 14.0 (O=CHC(*Me*)=). Anal. Calcd for $MoC_{50}H_{34}N_6B_2O_2F_{24}\cdot 0.5CH_2Cl_2$ (CH_2Cl_2 determined by ^{1}H NMR): C, 44.38; H, 2.58; N, 6.15. Found: C, 44.66; H, 2.72; N, 6.32.

[TpMo(CO)(MeC≡CMe)(η^1-O=CHPh)][BAr′$_4$] (8d): brown powder, green crystals; 78% yield; IR (CH_2Cl_2) 1977 ($\nu_{C\equiv O}$) cm^{-1}; ^{1}H NMR (CD_2Cl_2) δ 8.53 (s, 1 H, C*H*O), 7.60−7.47 (m, obscured by *p*-Ar′, 5 H, O=CH*Ph*); ^{13}C{H} NMR (CD_2Cl_2) δ 199.1 (*C*=O), 139.1 (*p* of Ph), 133.4 (*ipso* of Ph), 132.0, 130.2 (*o, m* of Ph). Anal. Calcd: C, 46.79; H, 2.52; N, 6.18. Found: C, 46.73; H, 2.52; N, 6.22.

[TpMo(CO)(MeC≡CMe)(η^1-*p*-O=CHC$_6$H$_4$Me)][BAr′$_4$] (8e): brown powder, green crystals; 80% yield; IR (CH_2Cl_2) 1970 ($\nu_{C\equiv O}$) cm^{-1}; ^{1}H NMR (CD_2Cl_2) δ 8.45 (s, 1 H, C*H*O), 7.41, 7.32 (each a d, each 2 H, J_{HH} = 8.5 Hz each, C$_6$*H*$_4$), 2.46 (s, 3 H, C$_6$H$_4$−*Me*); ^{13}C{H} NMR (CD_2Cl_2) δ 199.2 (*C*=O), 152.4 (*C*−Me of C$_6$H$_4$), 132.3 (br, *C*$_6$H$_4$), 131.3 (*ipso* of C$_6$H$_4$), 131.1 (br, *C*$_6$H$_4$), 22.5 (C$_6$H$_4$−*Me*). Anal. Calcd: C, 47.19; H, 2.64; N, 6.11. Found: C, 47.11; H, 2.69; N, 6.18.

Acknowledgment. We gratefully acknowledge the National Science Foundation (Grant No. CHE-9727500) for support of this research.

Supporting Information Available: This material is available free of charge via the Internet at http://pubs.acs.org.

OM990864X